Original Article

CLCA1 and BPIFB1 are potential novel biomarkers for asthma: an iTRAQ analysis

Tianci Chai[1], Yinji Liu[1], Yuwei Zeng[1], Sung-Yoon Kang[2], Jie Li[1]

[1]Key Laboratory of Shenzhen Respiratory Disease, Shenzhen Institute of Respiratory Disease, Shenzhen People's Hospital (The First Affiliated Hospital of Southern University of Science and Technology, The Second Clinical Medical College of Jinan University), Shenzhen, China; [2]Division of Pulmonology and Allergy, Department of Internal Medicine, Gachon University Gil Medical Center, Incheon, Korea

Contributions: (I) Conception and design: J Li, T Chai; (II) Administrative support: J Li, T Chai; (III) Provision of study materials or patients: All authors; (IV) Collection and assembly of data: All authors; (V) Data analysis and interpretation: J Li, T Chai; (VI) Manuscript writing: All authors; (VII) Final approval of manuscript: All authors.

Correspondence to: Jie Li, PhD. Key Laboratory of Shenzhen Respiratory Disease, Shenzhen Institute of Respiratory Disease, Shenzhen People's Hospital (The First Affiliated Hospital of Southern University of Science and Technology, The Second Clinical Medical College of Jinan University), 1017 Dongmen North Road, Luohu District, Shenzhen 518020, China. Email: ljszry2018@126.com.

Background: Asthma is a chronic respiratory disease that affects billions of people. Due to its diverse phenotypes and endotypes with distinct pathophysiological mechanisms, significant challenges arise in its clinical diagnosis and treatment. The discovery of potential biomarkers of asthma has significant implications for its clinical classification and precise treatment. The purpose of this study is to identify potential biomarkers for asthma, providing a foundation for its diagnosis and treatment.

Methods: We constructed an ovalbumin (OVA)-sensitized asthmatic mice model and used isobaric Tags for Relative and Absolute Quantitation (iTRAQ) labeling and liquid chromatography-mass spectrometry/mass spectrometry (LC-MS/MS) technology to identify differentially expressed proteins (DEPs) in lung tissues. We then performed enrichment analyses of the DEPs using the Gene Ontology (GO) and Kyoto Encyclopedia of Genes and Genomes (KEGG) databases, and constructed protein-protein interaction (PPI) networks.

Results: We identified 242 DEPs in the asthmatic mice model and showed that heat shock protein family A (Hsp70) member 5 (HSPA5) is a central protein in asthma. Consistent with our bioinformatics analysis, our western blot validation confirmed that the protein levels of arginase 1 (ARG1), chitinase-like protein 3 (CHIL3), chloride channel accessory 1 (CLCA1), and bactericidal/permeability-increasing protein (BPI) fold-containing family B member 1 (BPIFB1) were significantly increased in asthma group compared to the control group. Thus, we found that CLCA1 and BPIFB1 were the most promising potential biomarkers of asthma.

Conclusions: Our iTRAQ analysis and western blot verification of asthmatic mice showed that HSPA5 is a central protein in asthma, and CLCA1 and BPIFB1 are novel potential biomarkers that could play significant roles in the diagnosis and treatment of asthma.

Keywords: Asthma; isobaric Tags for Relative and Absolute Quantitation (iTRAQ); biomarkers; BPIFB1; CLCA1

Submitted Aug 23, 2024. Accepted for publication Oct 04, 2024. Published online Oct 28, 2024.
doi: 10.21037/jtd-24-1366
View this article at: https://dx.doi.org/10.21037/jtd-24-1366

Introduction

Asthma is a chronic inflammatory respiratory disease. The interaction of many cells from both the innate and adaptive immune systems and epithelial cells leads to airway inflammation, bronchial hyper-reactivity, airway narrowing, airway remodeling, and heightened sensitivity (1-3). Asthma affects over 300 million people, and its clinical symptoms primarily include abnormal sensitivity to non-specific stimuli, such as cold air and exercise, which often results in recurrent shortness of breath and chest tightness (4-6). In contrast to the previously simplified clinical categorization of allergic asthma and non-allergic asthma (7,8), it is now recognized that different asthma phenotypes exhibit distinct pathophysiological characteristics; thus, more refined asthma endotype diagnosis, treatment, and research is required (9-11). These asthma endotypes differ in terms of genetic susceptibility, environmental risk factors, age of onset, clinical presentation, prognosis, and response to standard and new therapies. Thus, the identification of biomarkers specific to different endotypes is increasingly important for asthma diagnosis and treatment.

Proteomics is a research tool of significant scale that provides comprehensive data on protein expression patterns. It is widely employed to investigate the molecular mechanisms of complex biological mixtures, including traditional Chinese medicine (12,13). During disease states, protein expression undergoes dynamic changes in a spatiotemporal manner, regulated by post-transcriptional and chemical modifications. These modifications are highly relevant to the diagnosis and treatment of diseases. The application of emerging proteomics technologies has enabled the biological medium of serum/plasma to be used to study the etiology of asthma, identify diagnostic biomarkers, and explore drug targets in contemporary medicine (14-16). Proteomic analysis has enhanced our comprehension of asthma allergens and clinical treatment effects, and even facilitated personalized therapy (15,17). Compared to previous techniques like comparative two-dimensional (2D) gel electrophoresis and isotope-coded affinity tags (18), isobaric Tags for Relative and Absolute Quantitation (iTRAQ) combined with liquid chromatography-mass spectrometry/mass spectrometry (LC-MS/MS) is more sensitive, automated, and multidimensional. It has been successfully employed to detect a wide range of molecules (>20 kDa) and is better suited for studying the pathogenesis and pathophysiology of diseases (19-21).

We induced asthma in ovalbumin (OVA)-sensitized mice and used the multidimensional protein identification technology strategy, combining iTRAQ labeling and 2D LC-MS/MS, to identify the proteins that differed between the asthmatic and normal mice. We also performed Gene Ontology (GO) and Kyoto Encyclopedia of Genes and Genomes (KEGG) enrichment and pathway analyses and constructed a protein-protein interaction (PPI) network to identify potential asthma biomarkers. Our results were validated by western blot. We present this article in accordance with the MDAR and ARRIVE reporting checklists (available at https://jtd.amegroups.com/article/view/10.21037/jtd-24-1366/rc).

Highlight box

Key findings

- We identified a total of 242 differentially expressed proteins (DEPs), of which, 184 were upregulated and 58 were downregulated. Through a bioinformatics analysis of the DEPs, including Gene Ontology (GO) and Kyoto Encyclopedia of Genes and Genomes (KEGG) enrichment analyses, and the construction of a protein-protein interaction (PPI) network, we identified heat shock protein family A (Hsp70) member 5 (HSPA5) as a central protein in asthma. A validation via a Western blot analysis revealed that chloride channel accessory 1 (CLCA1) and bactericidal/permeability-increasing protein (BPI) fold-containing family B member 1 (BPIFB1) could serve as potential biomarkers for asthma.

What is known, and what is new?

- Asthma is a chronic respiratory disease impacting billions globally, marked by diverse phenotypes and endotypes. Identifying key biomarkers is essential for effective diagnosis and treatment.
- The present study identified 242 DEPs by comparing an asthmatic mice model to a wild-type mice model. Through the GO and KEGG enrichment analyses and the Search Tool for the Retrieval of Interacting Genes/Proteins (STRING) database, this study showed that HSPA5 is a central protein in asthma. Moreover, the potential biomarkers of asthma (i.e., CLCA1 and BPIFB1) were validated by western blot.

What is the implication, and what should change now?

- The discovery of these biomarkers could enable the more comprehensive diagnosis of asthma and targeted interventions to prevent its progression. Future clinical trials should validate the efficacy of these biomarkers in diagnosing, treating, and monitoring asthma.

Methods

Mice

We used 6-week-old female BALB/C mice from the

Guangdong Provincial Medical Experimental Animal Center for the animal experiments. All the animal procedures were approved by the ethics committee of Shenzhen People's Hospital (The First Affiliated Hospital of Southern University of Science and Technology, The Second Clinical Medical College of Jinan University) (No. SUSTC-JY2020054) and followed the national guidelines for the care and use of laboratory animals. A protocol was prepared before the study without registration. Every effort was made to minimize animal suffering and reduce the number of mice used.

Animal sensitization and airway challenge

The BALB/C mouse group (n=6) was sensitized and challenged randomly. Sensitization was induced by an intraperitoneal injection of 20 μg of grade V OVA, mixed with 50 μL of 30 mg/mL Inject® Alum (Thermo Fisher Scientific, catalog number: 77161), on days 0, 14, 28. Subsequently, the challenge involved three weekly exposures of 30 minutes each to 5% grade II OVA, beginning from day 2 continuing for a period of six weeks. The control group (n=10) was similarly treated with physiological saline (Biosharp, catalog number: BL158A). The mice were sacrificed 24 hours following their final exposure to OVA or saline.

Protein extraction and enrichment

After mixing the samples, they were placed in a pre-chilled mortar and ground with liquid nitrogen until the tissue turned into fine powder without any visible particles. The powder was then dissolved and washed thoroughly using lysis buffer L3 Sodium dodecyl sulfate (SDS) (7 M urea, 2 M thiourea, 20 mM tris base, 0.2% SDS) and transferred to a new Eppendorf (EP) tube. The sample was subjected to sonication (80 w, 0.8 s on, and 0.8 s off, with 10 cycles on ice), followed by centrifugation at 4 ℃, 12,000 rpm for 20 minutes to collect the supernatant. Each tube containing 250 μL of the supernatant was mixed with 1 mL of acetone at –20 ℃ and precipitated overnight. The next day, the mixture was centrifuged at 4 ℃, 12,000 rpm for 20 minutes, the supernatant was discarded, and the pellet was air-dried on a calm surface and stored at –80 ℃ awaiting future use.

After drying, 100 μL of lysis buffer L3 (7 M urea, 2 M thiourea, 20 Mm tris base) was added to the protein pellet. The mixture was dispersed by pipetting until the protein was fully solubilized, after which sonication was performed (80 w, 0.8 s on, and 0.8 s off, with four cycles at 4 ℃). The sample was centrifuged at 12,000 rpm for 20 minutes at 4 ℃ to collect the enriched protein supernatant.

Protein quantification and enzymatic digestion

The Bradford standard curve was prepared by vortexing and oscillating 2 μL of the sample in 1 mL of Bradford reagent (Thermo Fisher Scientific, catalog number: A55866) for 20 seconds until thoroughly mixed. The absorbance values were measured, and the concentrations of each piece were calculated and adjusted accordingly.

A fixed amount of 200 μg of protein was mixed with 4 μL of tris(2-carboxyethyl) phosphine (TCEP) reducing reagent(AB Sciex, catalog number 4381664). The reaction was conducted at 60 ℃ for 1 hour to reduce the protein disulfide bonds. Next, 2 μM of methyl methanethiosulfonate (MMTS) cysteine-blocking reagent (AB Sciex, catalog number 4381664) was added at room temperature for 30 minutes to perform alkylation. Next, the mixture was transferred to a 10 K-ultrafiltration tube (Pall, catalog number: OD010C33) and centrifuged at 12,000 rpm for 20 minutes. The bottom solution in the collection tube was discarded, and 10 0 μL of 8 M urea (pH 8.5) was added. The tube was centrifuged at 12,000 rpm for 20 minutes, and the bottom solution was discarded. This process was repeated twice to remove small molecular substances. Next, 0.25 M tetraethylammonium bromide (TEAB) (pH 8.5) (Sigma, catalog number: T418) was added to the ultrafiltration tube and centrifuged at 12,000 rpm for 20 minutes. The bottom solution in the collection tube was discarded, and this step was repeated three times. A new collection tube was used, and 0.5M TEAB was added to the ultrafiltration tube to reach a final volume of 50 μL. The trypsin (Promega, catalog number: V5280) was added to the mixture at a ratio of 1:50 and incubated overnight at 37 ℃. The next day, the reaction was continued at 37 ℃ for 4 hours at a ratio of 1:100. The mixture was then centrifuged at 12,000 rpm for 20 minutes to collect the residue. The ultrafiltration tube was supplemented with 50 μL of 0.5M TEAB and centrifuged at 12,000 rpm for 20 minutes to combine with the previous fraction.

iTRAQ labeling and high-pH reverse-phase fractionation

According to the manufacturer's instructions, after isopropanol treatment, the 8-plex iTRAQ reagent kit (AB Sciex, catalog number 4381664) was added to a sample of

50 µL. The control group was divided into three groups, labeled 117, 119, and 121, while the asthma group was divided into three groups, labeled 114, 115, and 116. After a 2-hour reaction at room temperature, 100 µL of water was added to terminate the reaction. The mixed labeled samples were vortexed and centrifuged to the bottom of the tube, followed by vacuum centrifugation to dryness and subsequent freezing for storage.

Peptides labeled with iTRAQ were separated using a high-performance liquid chromatography (HPLC) system (Shimadzu, LC-2050). First, the peptides were reconstituted in solvent A, which comprised ammonium hydroxide (NH_3 in H_2O; pH =10) and water, and then loaded onto a Phenomenex C18 reverse-phase chromatography column (Gemini-NX 3 µ C18 110 Å; 150 mm × 2.00 mm) (AB Sciex, catalog number 4381664). Solvent B, with a gradient of 80% ammonium acetate (NH3 in H_2O; pH =10), was gradually increased from 5% to 37% over 5 minutes, followed by a final increase in the solvent B proportion to 95% and maintained for 5 minutes. The elution was performed for 85 minutes at a 0.2 mL/min flow rate. Detection was carried out using a 214-nm absorbance spectra, and 24 fractions were collected based on the peak shape from the linear gradient.

LC-MS/MS analysis

The peptide samples were dissolved in a solvent containing 0.1% formic acid and 5% acetonitrile, and then underwent vortexing and oscillation at 13,500 rpm, 4 ℃ for 20 minutes. In the 2D reversed-phase chromatography section, the Thermo Dionex Ultimate 3000 RSLCnano liquid phase system was used, employing a C18 capillary column (75 µm i.d. ×150 mm, packed with Acclaim PepMap RSLC C18, 2 µm, 100Å, nanoViper) (Thermo Fisher Scientific, catalog number: 164946) for separation. The mobile phase A comprised a 0.1% formic acid aqueous solution, while the mobile phase B comprised a 0.1% formic acid solution in 80% acetonitrile. The flow rate was set at 300 nl/min. The gradient elution program involved a linear increase in the concentration of mobile phase B from 5% to 35% over 40 minutes. The analysis time for each component was set at 65 minutes.

The separated samples were directly introduced into the Q Exactive quadrupole-orbitrap mass spectrometer (Thermo Fisher Scientific) for detection. The mass spectrometry (MS) was conducted using an electrospray ionization source in positive ion mode. The resolution of the first-level mass spectrometry (MS1) was set at 7 w, with an automatic gain control (AGC) target of 300 w, a maximum ion injection time of 100 ms, and a scanning range of 350–1,800 m/z. The resolution of the second-level mass spectrometry (MS2) was set at 1.75 w, with an AGC target of 5 w, a maximum ion injection time of 120 ms, and a fragmentation energy of 30 for the first 20 precursor ions.

Protein identification

In the proteomics experiment, we employed AB Sciex's ProteinPilot (version 5.0) for the proteome analysis of the iTRAQ-labeled peptides. The parameter settings of the software were as follows: the protein threshold was set to unused protscore >0.05 (corresponding to a false positive rate below 10%); and the competing protein error range was set to 2.0. The mouse protein database used was Mouse_TrSp_UniProt_2017.3.30.fasta. A thorough search mode was applied, and a false discovery rate (FDR) analysis was performed. The analysis was carried out using the Paragon algorithm (version 5.0.1.0) and the default parameters provided by the ProteinPilot software.

The screening and visualization of the DEPs

According to the official instructions provided by AB SCIEX, we employed the ProteinPilot™ software for the MS data retrieval and conducted an FDR analysis to identify potential false positives. After the completion of the retrieval process, we proceeded to filter and refine the retrieved results (iTRAQ raw data). We used the unused value as a reliability indicator for the protein identification, setting an unused threshold value ≥1.3 to ensure a reliability level of 95% or higher for the selected protein identifications. Additionally, we eliminated the records corresponding to the reversed databases and those starting with "RRRRR", and excluded proteins with poor reproducibility based on the coefficient of variation. Through these aforementioned steps, we obtained a reliable set of proteins.

We calculated the $\log_2$(fold change) values and performed *t*-tests with the Benjamini-Hochberg correction for the reliable proteins to compare the asthmatic mice group to the control group. We identified the differentially expressed proteins (DEPs) in the asthmatic group by selecting proteins with a $\log_2$(fold change) >2 and a P adjusted value ≤0.5. Further, we conducted the visualization analysis using the "ggplot" package in R Studio (version 2022.07.02 Build 576, R version 4.3.0).

GO and KEGG analyses of the DEPs

We performed the GO enrichment analysis using the "org.Mm.eg.db" (version 3.17.0) package and the "clusterProfiler" (version 4.8.1) package in R Studio. The "enrichGO" function was employed to investigate the genes corresponding to the DEPs in terms of their molecular functions (MFs), cellular components (CCs), and biological processes (BPs). Additionally, we conducted a KEGG pathway analysis using the "enrichKEGG" function to explore the pathways associated with the DEPs.

PPI network analysis

We imported the DEPs into the Search Tool for the Retrieval of Interacting Genes/Proteins (STRING) database for mapping to obtain information about the interactions between the DEPs, and we identified the PPI pairs with a comprehensive score >4.0. A PPI network analysis was performed online (https://string-db.org/). Subsequently, the PPI network was visualized using Cytoscape software (http://www.cytoscape.org/, version 3.9.1), and the central proteins with high betweenness centrality (BC) were selected using the "cytohubba" and "cytoNCA" plugins.

Western blot

The sample concentration adjustment was performed after the bicinchoninic acid assay quantification. Sodium dodecyl-sulfate polyacrylamide gel electrophoresis was carried out at constant voltages of 80 and 120 V for 20 and 60 minutes, respectively, to separate the proteins. The proteins were then transferred onto methanol-activated polyvinylidene difluoride membranes (0.45 μm) using the "sandwich model" and transferred at a constant current of 200 mA for 75 minutes in an ice bath. The membranes were incubated with 5% bovine serum albumin (BSA) at room temperature for 60 minutes, followed by overnight incubation at 4 ℃ with primary antibodies against arginase 1 (ARG1) (sc-47715, Santa Cruz), chitinase-like protein 3 (CHIL3) (ab192029, Abcam), chloride channel accessory 1 (CLCA1) (ab180851, Abcam), and bactericidal/permeability-increasing protein (BPI) fold-containing family B member 1 (BPIFB1) (ab219098, Abcam). The membrane was washed three times with tris-buffered saline with tween (TBST) at room temperature and then incubated for 60 minutes with a secondary antibody containing horseradish peroxidase (HRP). The membranes were washed three times with TBST and visualized using the Thermo Scientific SuperSignal West Pico PLUS (Thermo Fisher, catalog number 34580). The images were captured using the Image LAS 500 imaging system.

Statistical analysis

The data are presented as the mean ± standard error of the mean. The statistical analysis was performed using a one-way analysis of variance, followed by Dunnett's post-hoc test to ascertain statistical significance. P value less than 0.05 was considered statistically significant.

Results

Protein profiling

A total of 4,996 credible proteins were identified by iTRAQ MS (available online: https://cdn.amegroups.cn/static/public/10.21037jtd-24-1366-1.csv). These proteins exhibited a high confidence level of over 95% and had a significantly high protein sequence coverage. Among them, 64% of the proteins had a coverage exceeding 10%, while 7.3% of the proteins had a coverage exceeding 50% (*Figure 1A*). The majority of the identified proteins contained less than 10 peptide segments, and the number of identified proteins decreased as the number of matched peptide segments increased (*Figure 1B*).

We selected the proteins with a $\log_2$(fold change) >1 and <–1 as the DEPs in the asthma group. A total of 242 DEPs were identified, of which, 184 were upregulated, and 58 were downregulated (available online: https://cdn.amegroups.cn/static/public/10.21037jtd-24-1366-2.csv). These findings are visually depicted in a volcano plot (*Figure 1C*). Further, a hierarchical clustering analysis of these DEPs was performed, demonstrating excellent data reproducibility (*Figure 1D*).

GO and KEGG enrichment analyses of the DEPs

We performed a GO functional enrichment analysis of the DEPs, comparing the lung tissue of the asthmatic mice to that of the wild-type mice. The results revealed a total enrichment of 728 terms in the set of differentially expressed genes (DEGs) (available online: https://cdn.amegroups.cn/static/public/10.21037jtd-24-1366-3.csv). Among them, 495 terms were enriched in BPs, 103 terms in CCs, and 130 terms in MFs. To showcase the GO enrichment

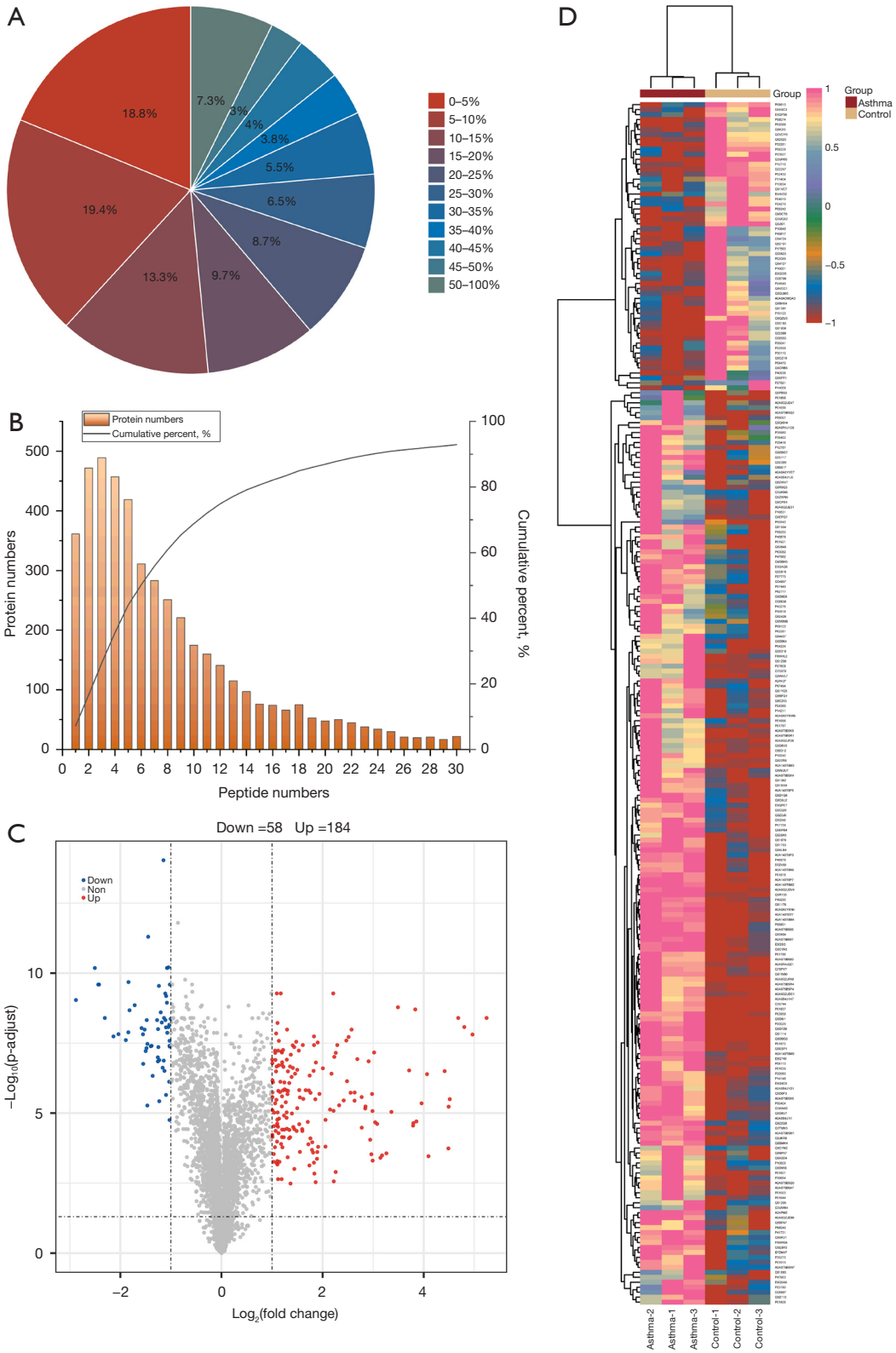

Figure 1 Protein profiling. (A) Distribution of protein sequence coverage. (B) Peptide number distribution. (C) Volcano plots of proteins for asthma and control groups. (D) Heatmap of DEPs. DEPs, differentially expressed proteins.

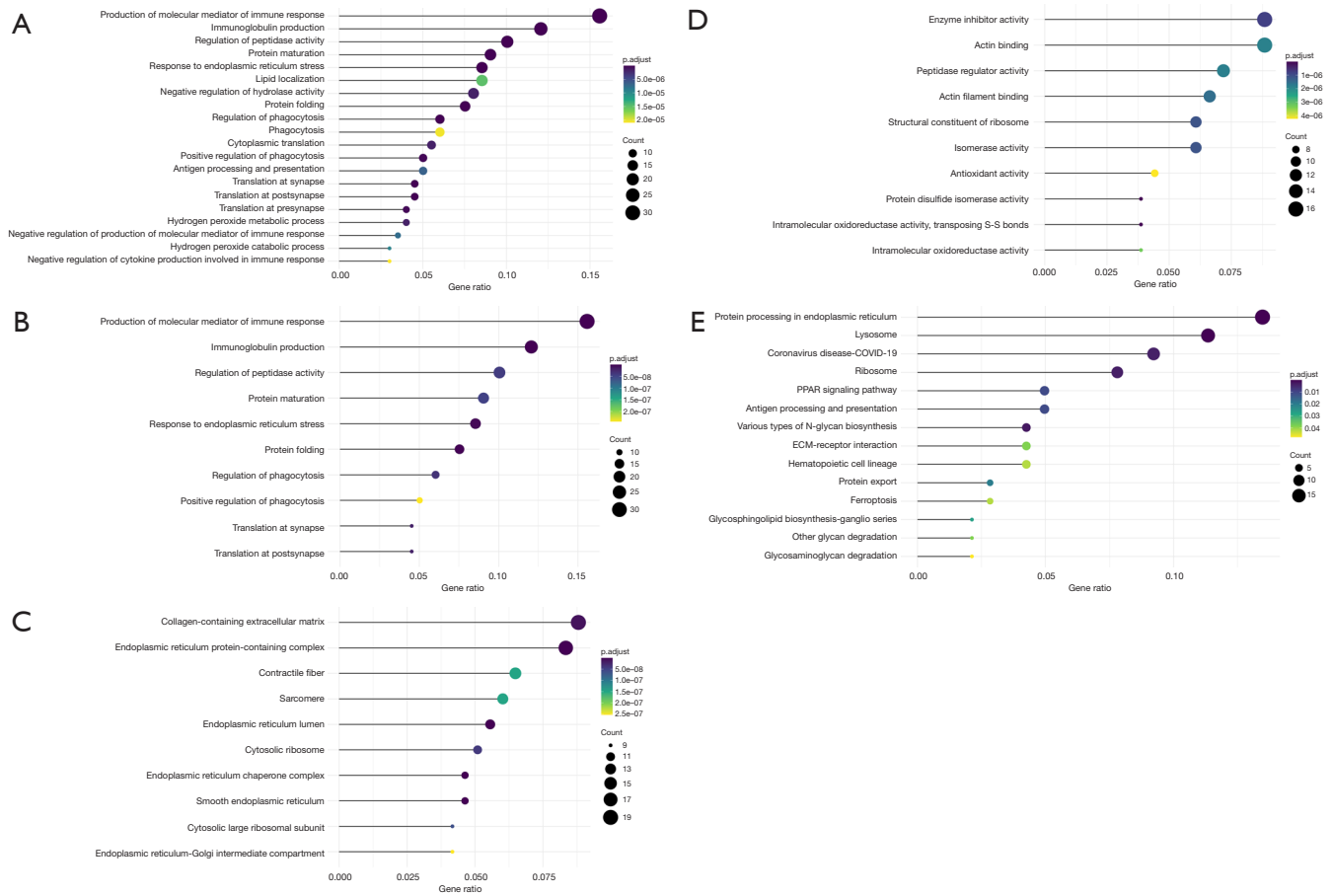

Figure 2 GO and KEGG enrichment analyses of the DEPs. (A) Top 20 GO enrichment terms of the DEPs. (B) Top 10 GO enrichment terms for the BP of the DEPs. (C) Top 10 GO enrichment terms for the CCs of the DEPs. (D) Top 10 GO enrichment terms for MFs of the DEPs. (E) KEGG enrichment terms of the DEPs. COVID-19, coronavirus disease 2019; PPAR, peroxisome proliferator-activated receptor; ECM, extracellular matrix; GO, Gene Ontology; KEGG, Kyoto Encyclopedia of Genes and Genomes; DEPs, differentially expressed proteins; BP, biological process; CC, cellular component; MF, molecular function.

results, the top 20 terms were selected. Notably, the DEGs in the asthmatic mouse DEPs were predominantly associated with the production of molecular mediators of the immune response (GO:0002440), immunoglobulin production (GO:0002377), and regulation of peptidase activity (GO:0052547) (*Figure 2A*). Conversely, in the BP category, the major focus was on the production of molecular mediators of immune response (GO:0002440), immunoglobulin production (GO:0002377), and regulation of peptidase activity (GO:0052547) (*Figure 2B*). In terms of the CCs, the main focus was on the collagen-containing extracellular matrix (ECM) (GO:0062023), endoplasmic reticulum protein-containing complex (GO:0140534), and contractile fiber (GO:0043292) (*Figure 2C*). In terms of the MFs, the primary emphasis was on enzyme inhibitor activity (GO:0004857), actin binding (GO:0003779), and peptidase regulator activity (GO:0061134) (*Figure 2D*). Additionally, our results also revealed a significant association between these DEPs and coronavirus disease 2019 (COVID-19).

We performed a KEGG enrichment analysis of the DEPs in the asthmatic mice (*Figure 2E*). Our findings revealed that the signaling pathways of these DEPs mainly focused on protein processing in the endoplasmic reticulum (mmu04141), the peroxisome proliferator-activated receptor (PPAR) signaling pathway (mmu03320), ECM-receptor interaction (mmu04512), antigen processing and presentation (mmu04612), and ferroptosis (mmu04216) (available online: https://cdn.amegroups.cn/static/public/10.21037jtd-24-1366-4.csv). These pathways revealed an association between asthma and immune

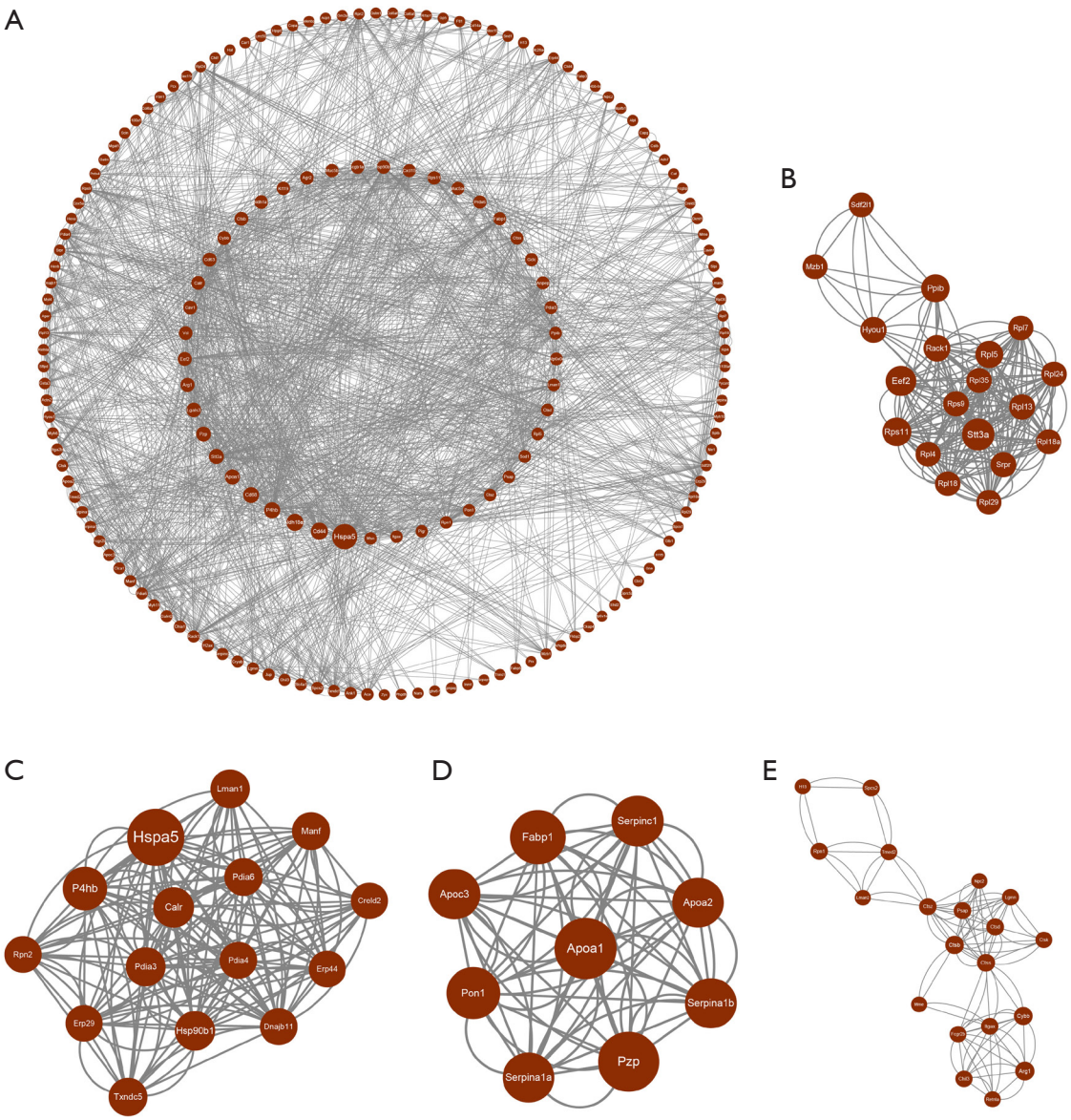

Figure 3 PPI of DEPs. (A) The interaction networks of all the DEPs. (B-E) Top four high scores based on a cluster analysis by "MCODE", a plugin of Cytoscape. PPI, protein-protein interaction; DEPs, differentially expressed proteins.

responses, such as the secretion of inflammatory factors like interleukin (IL)-4, IL-5, IL-13 and the presentation and processing of cluster of differentiation (CD)4$^+$ or CD8$^+$ T cell antigens. PPARs and ferroptosis also emerged as aspects highly relevant to the pathogenesis of asthma.

PPI of the DEPs

To examine the potential molecular mechanisms of the DEPs in the pathogenesis of asthma, we constructed a protein-protein co-expression network of the DEPs using the STRING database and Cytoscape software. After removing non-edge connecting nodes, the PPI network comprised a total of 172 nodes and 877 edges. Subsequently, we calculated the betweenness (BC) scores and arranged them in descending order (*Figure 3A*). The top 10 proteins were as follows: heat shock protein family A (Hsp70) member 5 (HSPA5), CD44, ALDH18A1, P4HB, CD68, APOA1, STT3A, PZP, LGALS3, and ARG1 (available online: https://cdn.amegroups.cn/static/

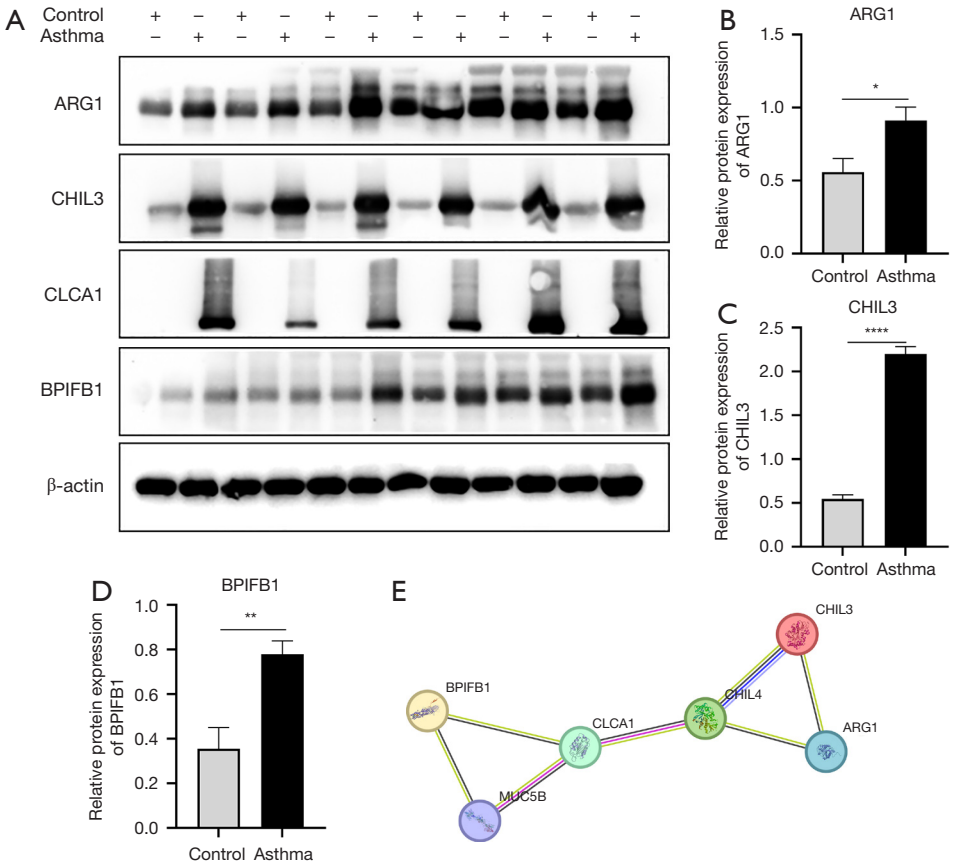

Figure 4 Validation of the DEPs. (A) Validation of four important proteins in asthma (i.e., ARG1, CHIL3, CLCAl, BPIFB1). (B-D) The relative protein levels of AGR1, CHIL3, and BPIFB1. (E) Interactions among ARG1, CHIL3, CLCA1, and BPIFB1 in the STRING database. *, P<0.05; **, P<0.01; ****, P<0.0001. DEPs, differentially expressed proteins; ARG1, arginase 1; CHIL3, chitinase-like protein 3; CLCAl, chloride channel accessory 1; BPIFB1, bactericidal/permeability-increasing protein (BPI) fold-containing family B member 1.

public/10.21037jtd-24-1366-5.csv). Consistent with our GO enrichment findings, the results showed that HSPA5 was a pivotal hub protein, localized in the endoplasmic reticulum, and extensively involved in immunoglobulin binding processes. Further, we performed additional analyses on the co-expression network using the "MCODE" plugin in Cytoscape to identify potential key modules. We identified four important modules (*Figure 3B-3E*). The first of these modules, which comprised 19 nodes and 230 edges, had the highest score. Interestingly, HSPA5 reappeared in the second-highest scoring module, which comprised 15 nodes and 174 edges. These results suggest that HSPA5 plays a crucial role in the pathogenesis of asthma.

Validation of the DEPs

To validate the reliability of the iTRAQ data, we selected four DEPs with crucial functions. The expression levels of the proteins (i.e., ARG1, CHIL3, CLCA1, and BPIFB1) were quantitatively analyzed by Western blot. These proteins exhibited significant changes in expression levels in the iTRAQ profiling, and were closely associated with the inflammatory response and antigen delivery and expression in asthma. The validation results were consistent with the trends observed in the iTRAQ results. Notably, ARG1, CHIL3, CLCA1, and BPIFB1 showed a marked upregulation in the fold change results (asthma group/control group) (*Figure 4A*) with CLCA1 exhibiting the most significant difference. The grayscale values of the Western blot images were quantified, and relative quantification was performed (*Figure 4B-4D*). Additionally, we constructed a PPI network of these four proteins in the STRING database to reveal the potential interaction relationships among them (*Figure 4E*).

Discussion

Asthma is a prevalent chronic respiratory disease with a high global incidence, and affects the lives of millions of individuals. It exhibits complex phenotypes and endotypes, each with distinct pathophysiological mechanisms and necessitating different treatment approaches. Thus, the identification of biomarkers specific to different endotypes is of great importance in the diagnosis and management of asthma. Type 2 high asthma is commonly observed in allergic asthma. In the present study, we employed iTRAQ labeling combined with LC-MS/MS proteomic identification to screen for DEPs by comparing an OVA-sensitized asthmatic mice model group and a control group. The GO and KEGG enrichment analyses of these DEPs revealed their association with immune response and antigen presentation. By constructing a PPI network, we identified HSPA5 as a crucial hub protein in the pathogenesis of asthma. Finally, through the western blot analysis, we discovered that in addition to ARG1 and CHIL3, which have been widely reported to be involved in the mechanisms of asthma, CLCA1 and BPIFB1 could serve as potential novel biomarkers for asthma.

First, the GO enrichment analysis revealed that the genes encoding differential proteins were predominantly enriched in the regulation of the immune response. T helper cell type 2 (Th2)-type asthma is generally believed to be induced by exogenous allergens that drive the differentiation of $CD4^+$ T cells into Th2 cells that secrete pro-inflammatory cytokines such as IL-4, IL-5, and IL-13 (22,23). These cytokines can stimulate B cells to produce immunoglobulin E (IgE) antibodies, which then bind to the surface of effector cells such as mast cells and eosinophils. On re-exposure to the allergen, the allergen binds to the IgE antibodies, leading to the release of mediators such as histamine, leukotrienes, and prostaglandins by the effector cells. This results in inflammatory reactions, including bronchial smooth muscle contraction, increased mucus secretion, and increased vascular permeability, ultimately causing asthma attacks (24,25).

By constructing a PPI network, we found that HSPA5 (also known as Binding immunoglobulin protein or BiPS) has a strong association with orosomucoid-like protein (ORMDL) sphingolipid biosynthesis regulator 3 (ORMDL3), a gene implicated in the risk of childhood asthma located on chromosome 17q21 (26-28). The overexpression of human ORMDL3 in transgenic mice leads to spontaneous airway remodeling, increased mucus production, and enhanced responsiveness to methacholine-induced bronchoconstriction (29). Liu *et al.* found a close association between HSPA5, type I interferon response, and increased ORMDL3 expression (30). When the endoplasmic reticulum (ER) is under stress, HSPA5 is translocated to the cell surface, where it binds to various ligands and activates multiple intracellular signaling pathways. At the cell surface, HSPA5/BiP/GRP78 can play various functional roles in cell viability, proliferation, apoptosis, adhesion, and the regulation of both innate and adaptive immunity (31). Abnormalities in HSPA5 may lead to the aberrant activation of innate immunity, resulting in refractory asthma. Additionally, HSPA5 may be closely related to the airway hyperresponsiveness in asthma. On one hand, abnormalities in HSPA5 lead to endoplasmic reticulum stress, which may result in dysfunction of airway epithelial cells, thereby exacerbating airway hyperresponsiveness (32). On the other hand, HSPA5 may also be involved in the regulation of neurons (33), further enhancing the role of neuronal populations in allergen-induced airway contraction responses (34).

Among the proteins that we validated, ARG1 has been widely recognized as a biomarker for pediatric asthma (35,36). CHIL3 [also known as Ym1 or eosinophil chemotactic factor (ECF-L), a member of the chitinase-like protein (CLP) family] is a protein with chitinase-like properties but lacks chitinase activity (37-39). It is frequently associated with Ym2 and participates in the immune response of Th2-type asthma, playing a crucial role in allergic asthma and related diseases (40-42). We are particularly intrigued by the intricate properties of CLCA1 and BPIFB1. CLCA1 is a member of the calcium-sensitive chloride conductance protein family (43), and is the protein in our validation group that showed the most significant expression differences. Our results demonstrated highly significant changes in the fold change value and western blot bands of CLCA1 in the asthma group. Further, previous studies have showed that CLCA1 gene expression levels are significantly higher than normal levels in the airway epithelial cells and sputum cells of asthma patients (44,45). Jakiela *et al.* conducted a transcriptomic analysis of bronchoalveolar lavage fluid from patients with non-steroidal anti-inflammatory drug (NSAID)-exacerbated respiratory disease and NSAID-tolerant asthma, which also demonstrated the high expression of CLCA1 (46). CLCA1 not only regulates the expression of mucins but also participates in the innate immune response of inflammatory cells by binding to yet unidentified molecules, promoting

the production of cytokines and chemokines, which in turn leads to the development of asthma (47). Additionally, a signaling pathway has been identified in which human CLCA activates mitogen-activated protein kinase 13 (MAPK13) (also known as p38δ-MAPK) to stimulate MUC5AC mucin gene expression (48,49). Excessive mucus secretion is a hallmark characteristic of asthma and other mucous obstructive airway diseases with MUC5AC and MUC5B being the major glycoprotein components of mucus (50,51).

Another protein we validated, BPIFB1 [also known as the long palate, lung, and nasal epithelium clone 1 (LPLUNC1)], is also reported to be associated with the MUC5AC and MUC5B mucins. BPIFB1 contains two BPI domains that bind specifically to lipopolysaccharides (LPS) in the cell wall of gram-negative bacteria, and is aberrantly expressed in cancer tissues, such as nasopharyngeal and lung cancers, and regulates chronic infections and inflammation (52-54). Donoghue *et al.* examined the allelic effects of MUC5B QTL, conducted a phylogenetic analysis, and examined BPIFB1 gene knockout mice, and confirmed that BPIFB1 is a novel regulator of MUC5B (55). In 2023, the team further demonstrated the necessity of BPIFB1 in the normal mucociliary clearance in BPIFB1 knockout mice, identifying it as a critical component of the mouse mucociliary apparatus and a potential key protein constituent of the mucus network (56).

Clinical studies have also shown that BPIFB1 is significantly expressed the sputum of asthma patients (57,58). Moreover, CLCA1 and BPIFB1 are frequently co-expressed in inflammatory diseases (55,59,60), which is consistent with our findings from the STRING database search, indicating potential underlying interactions between them. However, the specific regulatory mechanisms and interactions between the two have not been reported and require further exploration. BPIFB1 and CLCA1, as key proteins associated with mucus secretion, also serve as important biomarkers for the clinical diagnosis of asthma. In clinical sputum samples, in addition to elevated eosinophil counts and serum IgE levels, the upregulation of BPIFB1 and CLCA1 can assist in diagnosing Th2-type asthma. These proteins provide critical reference points for assessing the severity of mucus secretion in patients (57,61). The peripheral blood eosinophil count is the gold standard for identifying airway inflammation, while FeNO is a non-invasive and convenient testing method primarily associated with allergic inflammation, effectively predicting the occurrence, progression, and acute exacerbation of asthma. Although these biomarkers play an important role in the assessment of airway inflammation, our research found that CLCA1 and BPIFB1 provide unique information regarding airway remodeling and mucociliary clearance function in asthma patients. This finding offers a more precise diagnosis and intervention plan for patients with severe airway remodeling and mucociliary clearance impairment, aiding in the improvement of patient management and treatment outcomes. Furthermore, study on the treatment of asthmatic mice with TH5487 has revealed its regulatory effect on CLCA1 expression, though the underlying mechanisms remain unclear (62). As our understanding of CLCA1 mechanisms advances, it may emerge as a significant therapeutic target.

Despite the analysis and validation of DEPs in the asthma group marked by iTRAQ, we propose that BPIFB1 and CLCA1 may serve as novel biomarkers for Th2-type asthma. However, the OVA-sensitized mouse model often focuses on acute responses over a short-term period, lacking longitudinal studies on chronic inflammation and long-term immune memory. For example, airway inflammation and airway hyperresponsiveness seem to resolve within weeks after the last antigen exposure. In contrast, inflammation in human asthma often persists, leading to a resurgence of symptoms upon re-exposure to allergens (63). Furthermore, given the complexity of asthma and the heterogeneity of its phenotypes and endotypes, we will also need to conduct functional assays and gene knockout studies for these proteins, alongside clinical research, to validate our findings.

Conclusions

By integrating an OVA-sensitized asthma model with iTRAQ and LC-MS/MS, we identified the central protein HSPA5 in asthmatic mice, along with the potential biomarkers CLCA1 and BPIFB1, which are highly expressed in lung tissues. The identification of these biomarkers provides a solid experimental foundation for the refined classification and personalized treatment of asthma.

Acknowledgments

Funding: This work was supported by the Project of Shenzhen Basic Research Plan (No. JCYJ20210324114205014), the Key Laboratory of Shenzhen Respiratory Disease (No. ZDSYS201504301616234), and the Shenzhen Clinical Research Center for Respiratory Diseases.

Footnote

Reporting Checklist: The authors have completed the MDAR and ARRIVE reporting checklists. Available at https://jtd.amegroups.com/article/view/10.21037/jtd-24-1366/rc

Data Sharing Statement: Available at https://jtd.amegroups.com/article/view/10.21037/jtd-24-1366/dss

Peer Review File: Available at https://jtd.amegroups.com/article/view/10.21037/jtd-24-1366/prf

Conflicts of Interest: All authors have completed the ICMJE uniform disclosure form (available at https://jtd.amegroups.com/article/view/10.21037/jtd-24-1366/coif). The authors have no conflicts of interest to declare.

Ethical Statement: The authors are accountable for all aspects of the work in ensuring that questions related to the accuracy or integrity of any part of the work are appropriately investigated and resolved. All the animal procedures were approved by the ethics committee of Shenzhen People's Hospital (The First Affiliated Hospital of Southern University of Science and Technology, The Second Clinical Medical College of Jinan University) (No. SUSTC-JY2020054) and followed the national guidelines for the care and use of laboratory animals.

References

1. Kay AB. Asthma and inflammation. J Allergy Clin Immunol 1991;87:893-910.
2. Lambrecht BN, Hammad H. The immunology of asthma. Nat Immunol 2015;16:45-56.
3. Han KI, Lee H, Kim BG, et al. The Impact of Bronchiectasis on the Clinical Characteristics of Non-Severe Asthma. Allergy Asthma Immunol Res 2024;16:291-9.
4. Papi A, Brightling C, Pedersen SE, et al. Asthma. Lancet 2018;391:783-800.
5. Miller RL, Grayson MH, Strothman K. Advances in asthma: New understandings of asthma's natural history, risk factors, underlying mechanisms, and clinical management. J Allergy Clin Immunol 2021;148:1430-41.
6. Holtjer JCS, Bloemsma LD, Beijers RJHCG, et al. Identifying risk factors for COPD and adult-onset asthma: an umbrella review. Eur Respir Rev 2023;32:230009.
7. Schatz M, Rosenwasser L. The allergic asthma phenotype. J Allergy Clin Immunol Pract 2014;2:645-8; quiz 649.
8. Peters SP. Asthma phenotypes: nonallergic (intrinsic) asthma. J Allergy Clin Immunol Pract 2014;2:650-2.
9. Anderson GP. Endotyping asthma: new insights into key pathogenic mechanisms in a complex, heterogeneous disease. Lancet 2008;372:1107-19.
10. Wu W, Bleecker E, Moore W, et al. Unsupervised phenotyping of Severe Asthma Research Program participants using expanded lung data. J Allergy Clin Immunol 2014;133:1280-8.
11. Zhu T, Ma Y, Wang J, et al. Serum Metabolomics Reveals Metabolomic Profile and Potential Biomarkers in Asthma. Allergy Asthma Immunol Res 2024;16:235-52.
12. Naba A. Ten Years of Extracellular Matrix Proteomics: Accomplishments, Challenges, and Future Perspectives. Mol Cell Proteomics 2023;22:100528.
13. Zhang L, Liang X, Takáč T, et al. Spatial proteomics of vesicular trafficking: coupling mass spectrometry and imaging approaches in membrane biology. Plant Biotechnol J 2023;21:250-69.
14. Nieto-Fontarigo JJ, González-Barcala FJ, Andrade-Bulos LJ, et al. iTRAQ-based proteomic analysis reveals potential serum biomarkers of allergic and nonallergic asthma. Allergy 2020;75:3171-83.
15. O'Neil SE, Sitkauskiene B, Babusyte A, et al. Network analysis of quantitative proteomics on asthmatic bronchi: effects of inhaled glucocorticoid treatment. Respir Res 2011;12:124.
16. Jeong HC, Lee SY, Lee EJ, et al. Proteomic analysis of peripheral T-lymphocytes in patients with asthma. Chest 2007;132:489-96.
17. Wu YQ, Cai YX, Chen XL, et al. Proteomic analysis reveals potential therapeutic targets for childhood asthma through Mendelian randomization. Clin Transl Allergy 2024;14:e12357.
18. Gygi SP, Rist B, Gerber SA, et al. Quantitative analysis of complex protein mixtures using isotope-coded affinity tags. Nat Biotechnol 1999;17:994-9.

19. Ross PL, Huang YN, Marchese JN, et al. Multiplexed protein quantitation in Saccharomyces cerevisiae using amine-reactive isobaric tagging reagents. Mol Cell Proteomics 2004;3:1154-69.
20. Chen X, Sun Y, Zhang T, et al. Quantitative Proteomics Using Isobaric Labeling: A Practical Guide. Genomics Proteomics Bioinformatics 2021;19:689-706.
21. Yang T, Jia Y, Ma Y, et al. Comparative Proteomic Analysis of Bleomycin-induced Pulmonary Fibrosis Based on Isobaric Tag for Quantitation. Am J Med Sci 2017;353:49-58.
22. Anderson GP, Coyle AJ. TH2 and 'TH2-like' cells in allergy and asthma: pharmacological perspectives. Trends Pharmacol Sci 1994;15:324-32.
23. Wills-Karp M. Immunologic basis of antigen-induced airway hyperresponsiveness. Annu Rev Immunol 1999;17:255-81.
24. Punnonen J, Aversa G, Cocks BG, et al. Role of interleukin-4 and interleukin-13 in synthesis of IgE and expression of CD23 by human B cells. Allergy 1994;49:576-86.
25. Hammad H, Lambrecht BN. The basic immunology of asthma. Cell 2021;184:1469-85.
26. Hendershot LM, Valentine VA, Lee AS, et al. Localization of the gene encoding human BiP/GRP78, the endoplasmic reticulum cognate of the HSP70 family, to chromosome 9q34. Genomics 1994;20:281-4.
27. Moffatt MF, Kabesch M, Liang L, et al. Genetic variants regulating ORMDL3 expression contribute to the risk of childhood asthma. Nature 2007;448:470-3.
28. James BN, Weigel C, Green CD, et al. Neutrophilia in severe asthma is reduced in Ormdl3 overexpressing mice. FASEB J 2023;37:e22799.
29. Miller M, Rosenthal P, Beppu A, et al. ORMDL3 transgenic mice have increased airway remodeling and airway responsiveness characteristic of asthma. J Immunol 2014;192:3475-87.
30. Liu YP, Rajamanikham V, Baron M, et al. Association of ORMDL3 with rhinovirus-induced endoplasmic reticulum stress and type I Interferon responses in human leucocytes. Clin Exp Allergy 2017;47:371-82.
31. Tsai YL, Ha DP, Zhao H, et al. Endoplasmic reticulum stress activates SRC, relocating chaperones to the cell surface where GRP78/CD109 blocks TGF-β signaling. Proc Natl Acad Sci U S A 2018;115:E4245-54.
32. Duan Q, Zhou Y, Yang D. Endoplasmic reticulum stress in airway hyperresponsiveness. Biomed Pharmacother 2022;149:112904.
33. Fukawa M, Shirai R, Torii T, et al. Extracellular HSPA5 is autocrinally involved in the regulation of neuronal process elongation. Biochem Biophys Res Commun 2023;664:50-8.
34. Su Y, Xu J, Zhu Z, et al. Brainstem Dbh(+) neurons control allergen-induced airway hyperreactivity. Nature 2024;631:601-9.
35. Litonjua AA, Lasky-Su J, Schneiter K, et al. ARG1 is a novel bronchodilator response gene: screening and replication in four asthma cohorts. Am J Respir Crit Care Med 2008;178:688-94.
36. Li H, Romieu I, Sienra-Monge JJ, et al. Genetic polymorphisms in arginase I and II and childhood asthma and atopy. J Allergy Clin Immunol 2006;117:119-26.
37. Jin HM, Copeland NG, Gilbert DJ, et al. Genetic characterization of the murine Ym1 gene and identification of a cluster of highly homologous genes. Genomics 1998;54:316-22.
38. Bussink AP, Speijer D, Aerts JM, et al. Evolution of mammalian chitinase(-like) members of family 18 glycosyl hydrolases. Genetics 2007;177:959-70.
39. Chang NC, Hung SI, Hwa KY, et al. A macrophage protein, Ym1, transiently expressed during inflammation is a novel mammalian lectin. J Biol Chem 2001;276:17497-506.
40. Sun YJ, Chang NC, Hung SI, et al. The crystal structure of a novel mammalian lectin, Ym1, suggests a saccharide binding site. J Biol Chem 2001;276:17507-14.
41. Muallem G, Hunter CA. ParadYm shift: Ym1 and Ym2 as innate immunological regulators of IL-17. Nat Immunol 2014;15:1099-100.
42. Draijer C, Robbe P, Boorsma CE, et al. Dual role of YM1+ M2 macrophages in allergic lung inflammation. Sci Rep 2018;8:5105.
43. Gruber AD, Elble RC, Ji HL, et al. Genomic cloning, molecular characterization, and functional analysis of human CLCA1, the first human member of the family of Ca2+-activated Cl- channel proteins. Genomics 1998;54:200-14.
44. Peters MC, Mekonnen ZK, Yuan S, et al. Measures of gene expression in sputum cells can identify TH2-high and TH2-low subtypes of asthma. J Allergy Clin Immunol 2014;133:388-94.
45. Woodruff PG, Boushey HA, Dolganov GM, et al. Genome-wide profiling identifies epithelial cell genes associated with asthma and with treatment response to corticosteroids. Proc Natl Acad Sci U S A 2007;104:15858-63.

46. Jakiela B, Soja J, Sladek K, et al. Bronchial epithelial cell transcriptome shows endotype heterogeneity of asthma in patients with NSAID-exacerbated respiratory disease. J Allergy Clin Immunol 2023;151:953-65.
47. Liu CL, Shi GP. Calcium-activated chloride channel regulator 1 (CLCA1): More than a regulator of chloride transport and mucus production. World Allergy Organ J 2019;12:100077.
48. Alevy YG, Patel AC, Romero AG, et al. IL-13-induced airway mucus production is attenuated by MAPK13 inhibition. J Clin Invest 2012;122:4555-68.
49. Lv X, Zheng L, Zhang T, et al. CLCA1 exacerbates lung inflammation via p38 MAPK pathway in acute respiratory distress syndrome. Exp Lung Res 2024;50:85-95.
50. Welsh KG, Rousseau K, Fisher G, et al. MUC5AC and a Glycosylated Variant of MUC5B Alter Mucin Composition in Children With Acute Asthma. Chest 2017;152:771-9.
51. Kirkham S, Kolsum U, Rousseau K, et al. MUC5B is the major mucin in the gel phase of sputum in chronic obstructive pulmonary disease. Am J Respir Crit Care Med 2008;178:1033-9.
52. Wei F, Tang L, He Y, et al. BPIFB1 (LPLUNC1) inhibits radioresistance in nasopharyngeal carcinoma by inhibiting VTN expression. Cell Death Dis 2018;9:432.
53. Nam BH, Moon JY, Park EH, et al. Antimicrobial activity of peptides derived from olive flounder lipopolysaccharide binding protein/bactericidal permeability-increasing protein (LBP/BPI). Mar Drugs 2014;12:5240-57.
54. Jin G, Zhu M, Yin R, et al. Low-frequency coding variants at 6p21.33 and 20q11.21 are associated with lung cancer risk in Chinese populations. Am J Hum Genet 2015;96:832-40.
55. Donoghue LJ, Livraghi-Butrico A, McFadden KM, et al. Identification of trans Protein QTL for Secreted Airway Mucins in Mice and a Causal Role for Bpifb1. Genetics 2017;207:801-12.
56. Donoghue LJ, Markovetz MR, Morrison CB, et al. BPIFB1 loss alters airway mucus properties and diminishes mucociliary clearance. Am J Physiol Lung Cell Mol Physiol 2023;325:L765-75.
57. Baines KJ, Simpson JL, Wood LG, et al. Sputum gene expression signature of 6 biomarkers discriminates asthma inflammatory phenotypes. J Allergy Clin Immunol 2014;133:997-1007.
58. Li J, Xu P, Wang L, et al. Molecular biology of BPIFB1 and its advances in disease. Ann Transl Med 2020;8:651.
59. Fernández-Blanco JA, Fakih D, Arike L, et al. Attached stratified mucus separates bacteria from the epithelial cells in COPD lungs. JCI Insight 2018;3:e120994.
60. Birnhuber A, Jandl K, Biasin V, et al. Pirfenidone exacerbates Th2-driven vasculopathy in a mouse model of systemic sclerosis-associated interstitial lung disease. Eur Respir J 2022;60:2102347.
61. Rosser F J, Yue M, Han Y Y, et al. Long-term PM 2.5 exposure and upregulation of CLCA1 expression in nasal epithelium from youth with asthma. Ann Am Thorac Soc 2024. [Epub ahead of print]. doi: 10.1513/AnnalsATS.202403-309OC.
62. Tanner L, Bergwik J, Bhongir RKV, et al. Pharmacological OGG1 inhibition decreases murine allergic airway inflammation. Front Pharmacol 2022;13:999180.
63. Aun MV, Bonamichi-Santos R, Arantes-Costa FM, et al. Animal models of asthma: utility and limitations. J Asthma Allergy 2017;10:293-301.

(English Language Editor: L. Huleatt)

Cite this article as: Chai T, Liu Y, Zeng Y, Kang SY, Li J. CLCA1 and BPIFB1 are potential novel biomarkers for asthma: an iTRAQ analysis. J Thorac Dis 2024;16(10):6955-6968. doi: 10.21037/jtd-24-1366